Coronagraphic Detection of Exosolar Planets with the James Webb Space Telescope

M. Clampin, M. Rieke, G. Rieke, R. Doyon, J. Krist, and JWST Science Working Group

1. Introduction

The James Webb Space Telescope (Gardner et al. 2006) will have the capability to make significant, early progress in extrasolar planet studies. The JWST instrument complement features several coronagraphs that will be able to conduct programs imaging debris disks, and conduct searches to directly detect gas giant exoplanets.

2. JWST Instrument Complement

JWST is not primarily designed to conduct coronagraphic observations. It's segmented mirror telescope architecture, as shown in Figure 1, generates considerable additional diffraction structure in the telescope's point spread function compared to that of a monolithic mirror. The JWST project has set a performance requirement of diffraction limited imaging at 2 μm. This is defined in terms of an allocation of 150 nm wavefront error at the NIRCam focal plane. This 150 nm allocation contains specific reserves, and the degree to which these reserves are utilized or re-allocated is likely to influence the final performance for high contrast imaging. However, the stability, freedom from atmospheric absorptions, and low infrared backgrounds for JWST in space offer unique advantages that make possible a range of applications that complement other approaches. JWST has a unique discovery space for imaging the thermal emission of Jovian planets because of its superb sensitivity at the wavelengths where this emission emerges.

Figure 1: The James Webb Space Telescope

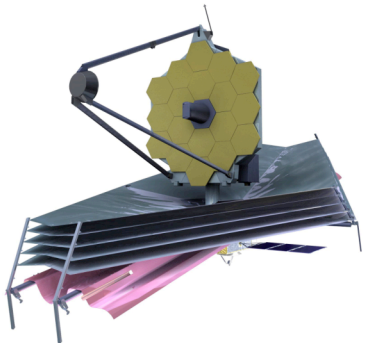

Figure 2: Preliminary occulter patterns for the NIRCam coronagraph. The five occulters are located on a transparent plate with clear areas of 20" x 20" each. Between the occulter fields are 5" x 5" neutral density squares to allow for the acquisition of bright stars. There are three radially-symmetric occulters with "sombrero" profiles scaled to match the given wavelengths for disk and extragalactic imaging. Two wedge-shaped occulters with sinc^2 profiles provide user-selectable widths, allowing for optimal imaging depending on wavelength.

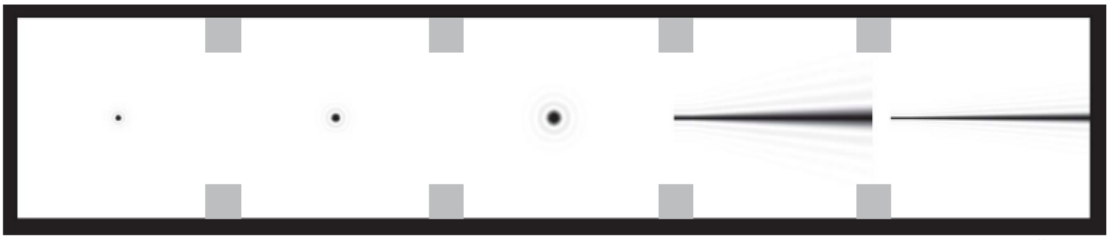

JWST's science payload comprises four science instruments (SI). NIRCam is a wide field, deep imaging camera that will also make the wavefront sensing and control (WFS&C) measurements, necessary to phase the telescope. NIRSpec is a multi-object spectrograph provided contributed by the European Space Agency (ESA). MIRI provides

mid-infrared (5-28.5 μm) imaging and spectroscopy. The Tunable Filter Imager (TFI) is a camera by the Canadian Space Agency. The three imagers each offer different coronagraphic capabilities to enable high contrast imaging.

Figure 3: Simulations by John Krist showing the mean *azimuthal contrast at which a signal-to-noise ratio of 5 detection of a planet around an M0V star at 4 pc is obtained in filter F460M with the wedge occulter. The corresponding planet masses and ages are shown on the right. The profiles are derived from roll-subtracted model images (20 nm RMS wavefront difference between rolls in addition to static aberrations) for both non-coronagraphic and coronagraphic observations. At each orientation, a 10000 sec exposure was obtained. The thick green line shows the contrast with the coronagraph (roll subtraction) with the sky background seen at Mauna Kea.*

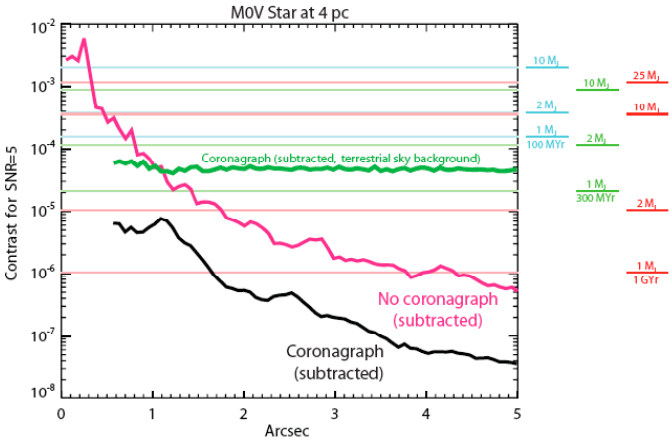

Figure 4: Simulated observations of a 1 GYr-old, M0V star at 4 pc with the NIRCam coronagraph (wedge occulter). Exposures of 5000 sec in each filter were taken at two orientations of the telescope separated by 10 deg. A 1 GYr-old, 2 MJ planet is shown at an apparent separation of 7 AU. Two field stars are also included: G2V (V=17.4) and M2V (V=18.0). (LEFT) Combined unsubtracted observations at the first orientation; (MIDDLE) Subtraction of F460M image taken at the second orientation from the first; (RIGHT) Multicolor subtracted images. The planet appears red because most of the flux is in the F460M filter.

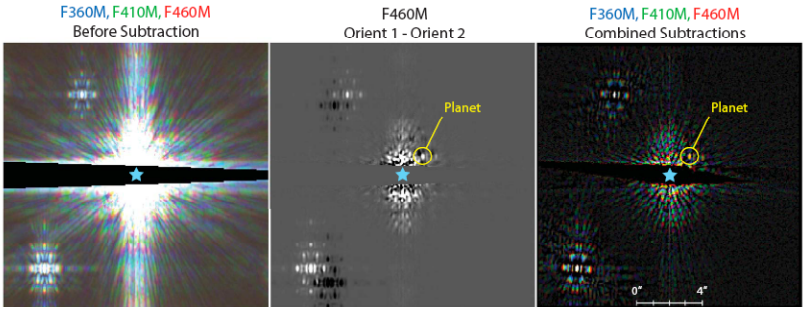

3 Coronagraphic Science with NIRCam

The NIRCam coronagraph permits coronagraphic imaging from 1 to 5 μm. Exact specifications for the occulting masks remain preliminary and will be optimized as the JWST optical design matures. The occulting masks currently baselined are shown in Figure 2. The focus in designing this complement has been exoplanet imaging at long wavelengths (4.5 μm)

3.2 Coronagraphic Performance

Figure 3 shows the NIRCam coronagraph's performance in detecting a M0V star at 4 pc, together with simulated images. NIRCam will be capable of imaging young, Jovian planets via their thermal emission, which peaks near λ=4.5 μm. At this wavelength, which is not easily accessible by ground-based telescopes due to the high IR background, the planet/star contrast ratio can be better than 10^{-5}. For comparison, in visible scattered light Jupiter appears 10^{-9} as bright as the Sun, impossible for any current telescope or JWST to see around another star.

Figure 5: NIRCam will be able to measure the effective temperatures of Jupiter-like planets very well as the plots below illustrate. The "data points" show the result of convolving Burrows et al. models with NIRCam filters to compute the two colors plotted. The color versus temperature relations were fit with simple polynomials and show that these two colors will pro vide temperature measurements.

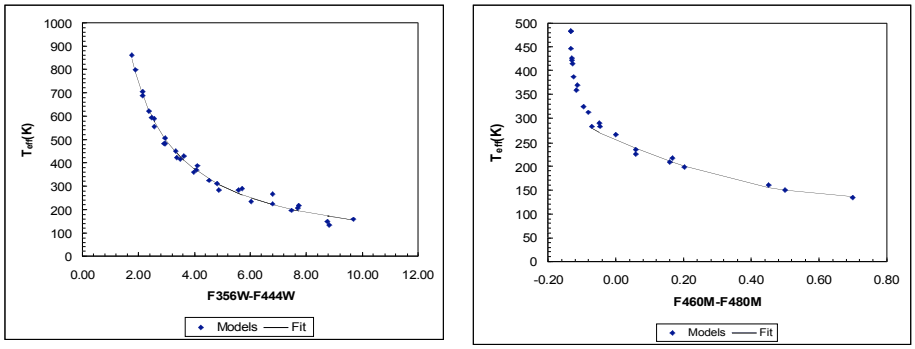

It is anticipated that most planet searches will use filter F460M and the wedge-shaped occulter, which provides the best performance. Observations at multiple roll angles will allow self-subtraction of the residual light from the star. Due to the characteristics of a planet's thermal emission spectrum, it will be possible to distinguish between planets and field stars by observing in one or two other filters. Due to the absence of atmospheric background, NIRCam will be superior to the largest current or planned ground-based telescopes for observations of thermal emission from Jupiter-mass planets at separations beyond ~0.6", and it will be able to see older Jupiters (up to 1 GYr). Targets for JWST observations will include the nearest M stars (<10 pc), young stars in nearby groups (10 MYr, 25-50 pc), and very young stars in the closest star forming regions (< 2MYr, <140 pc). Within 0.6" ground-based telescopes with extreme adaptive optics will be required (except for the youngest Jupiters around low-luminosity, nearby stars). NIRCam will be able to measure the effective temperatures of Jupiter-like planets very well as the plots in Figure 5 demonstrate.

4.0 Coronagraphic Science with the Tunable filter Imager (TFI)

TFI features an all-reflective optical design with a pick-off mirror (POM) at the telescope focus. The coronagraph is implemented through three circular Gaussian occulting spots (FWHM=0.75", 1.5", 2.0") plus one linear Gaussian occulter with a FWHM of 3" (Figure. 6). Each spot are spaced by 20" near the edge of the POM. The linear occulter is optimized for large (> 3") separations. All masks are manufactured as a random, yet deterministic, collection of 10-um diameter dimples (cones) directly engraved on the POM using diamond-turning technique. Since the incoming beam from the telescope hits

the POM at an angle of 18 degrees, the small cones act as small light traps, redirecting light off the f/20 beam. The net effect is to produce the desired tapered Gaussian profile.

Figure 6: TFI Occulting mask design

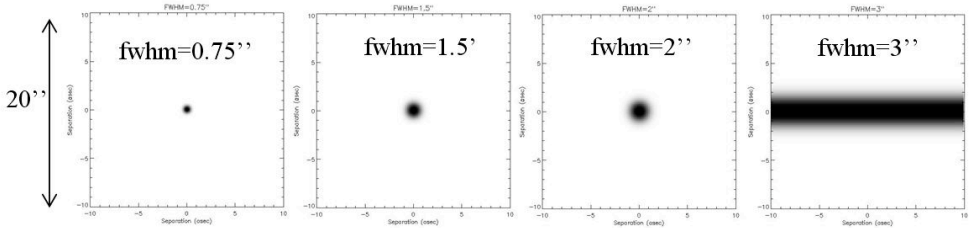

The occulting spots are combined with one of four apodized Lyot masks located in the pupil wheel. Unlike NIRCam, the TFI POM has no tip/tilt adjustment to correct for pupil shear between the telescope exit pupil and the instrument. To mitigate this potential problem, two of the Lyot masks have their shape and throughput optimized for a pupil shear of 1% (optimistic) and 3% (worst case). Similarly, two masks are optimized for the linear Gaussian occulter for two pupil shear scenarios. The Lyot mask designs are shown

Figure 7: TFI Lyot Stop design. The throughput varies from 22% to 55%.

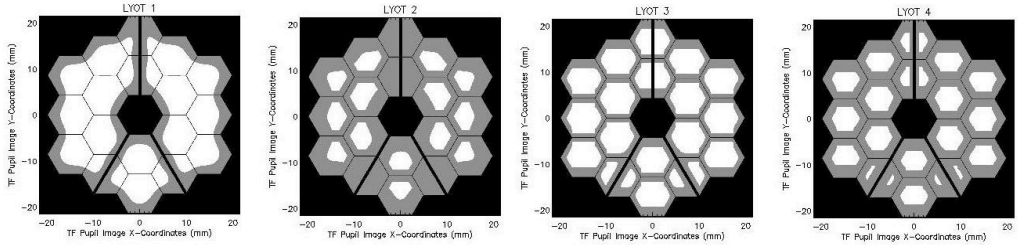

in Figure 7; their throughput ranges from 22% to 55%. Coronagraphic observations are possible over the full wavelength range of TFI (1.5-2.5; 3.1-5.0 μm) but the Lyot masks have been optimized at 4.6 μm where the discovery space is highest.

Figure 8: Contrast ratio at 4.6 μm. Photon and read-noise are not included. In practice, the TFI coronagraph is read-noise limited to a contrast floor of ~10^{-6} beyond ~2" on a *m'*=5 star assuming a cumulative exposure time of 1 hour.

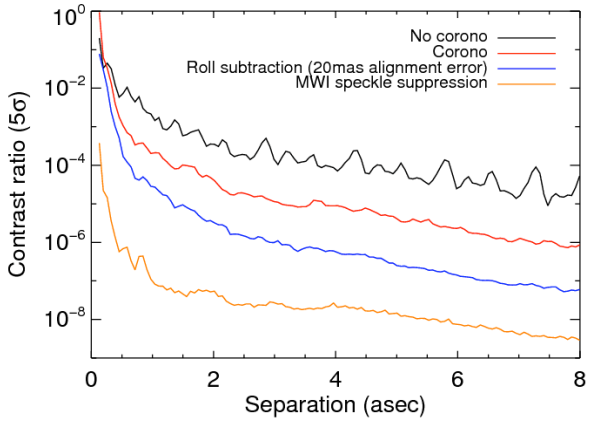

Figure 8 presents the nominal 5σ contrast performance (red curve) of the TFI coronagraph at 4.6 μm with the 2" occulting spot and a wavefront map with 130 nm RMS. The blue curve shows the improvement obtained through PSF subtraction (reference star(s)) or with roll; this case assumes (perhaps somewhat conservatively) 40 nm of differential low-order aberrations between the target and the reference plus a relative misalignment of 20 mas between the two observations. This offset is probably a worst case since the coronagraphic target acquisition accuracy is expected to be more like ~10 mas. This specific case yields a modest 10x contrast improvement. To illustrate that such performance is indeed modest, we note that quasi-

static speckle noise attenuation of ~100 is already achieved on ground based telescopes (Gemini & Keck) using optimal PSF subtraction algorithms such as angular differential imaging (Marois et al 2006 ; Lafrenière et al 2007). The relative thermal stability of L2 should enable very good point spread function calibration with JWST.

The wavelength scanning capability of TFI can be used to further suppress speckle noise using multi-wavelength imaging (MWI) speckle suppression algorithms (Marois et al 2000; Sparks & Ford 2002). The bottom (orange) curve in Figure 3 shows the theoretical performance obtained with MWI. The latter can yield speckle suppression factors as high as 100 but several effects (non-common path aberrations within the etalon, off-pupil optics) will likely conspire to reduce the efficacy of the technique.

Table 1 – Log_{10} of planet/star contrast at 4.6 µm (TFI Coronagraph)[1]

Sp	M_m	0.01 Gyrs			0.10 Gyrs			1 Gyrs			5 Gyrs		
		1 M_J	5 M_J	10 M_J	1 M_J	5 M_J	10 M_J	1 M_J	5 M_J	10 M_J	1 M_J	5 M_J	10 M_J
A0	0.78	-5.09	-4.16	-3.78	-5.96	-4.94	-4.47	-7.67	-5.83	-5.33	-8.87	-6.95	-5.97
F0	2.27	-4.49	-3.56	-3.18	-5.37	-4.35	-3.88	-7.07	-5.24	-4.74	-8.27	-6.36	-5.38
G2	3.58	-3.97	-3.04	-2.66	-4.84	-3.82	-3.35	-6.55	-4.71	-4.21	-7.75	-5.83	-4.85
K0	4.29	-3.68	-2.76	-2.38	-4.56	-3.54	-3.07	-6.26	-4.43	-3.93	-7.46	-5.55	-4.59
K5	4.69	-3.52	-2.60	-2.22	-4.40	-3.38	-2.91	-6.10	-4.27	-3.77	-7.30	-5.39	-4.41
M0	5.15	-3.34	-2.41	-2.03	-4.22	-3.20	-2.72	-5.92	-4.08	-3.58	-7.12	-5.20	-4.22
M5	7.98	-2.21	-1.28	-0.9	-3.08	-2.06	-1.59	-4.79	-2.95	-2.45	-5.99	-4.07	-3.09
L0	10.15	-1.34	-0.41	-0.03	-2.22	-1.20	-0.72	-3.92	-2.08	-1.58	-5.12	-3.22	-2.22
L5	10.98	-1.01	-0.08	0.30	-1.88	-0.86	-0.39	-3.59	-1.75	-1.25	-4.79	-2.88	-1.89
T0	11.40	-0.84	0.09	0.48	-1.72	-0.70	-0.22	-3.42	-1.58	-1.08	-4.62	-2.70	-1.72
T5	12.38	-0.45	0.48	0.86	-1.33	-0.31	0.16	-3.03	-1.20	-0.70	-4.23	-2.31	-1.34

Contrast exceeds the 10σ sensitivity beyond 1". [2]
Contrast exceeds the 10σ sensitivity beyond 5". [2]
Contrast exceeds the 10σ sensitivity beyond 1" *without* coronagraph and no PSF calibration.

[1] Evolutionary models from Barraffe *et al* 2003.
[2] Contrast threshold assuming the 2" (FWHM) occulting spot and a speckle noise attenuation factor ~10x achieved through reference star or roll (10σ version of the blue curve in Fig. 3). Potential gain obtained through a multi-wavelength imaging speckle suppression algorithm has been conservatively excluded. Note that read-noise imposes a contrast floor of ~10^{-6} (10σ) beyond ~ 2" for a cumulative exposure time of 1 hr on a *m'*=5 star.

Atmosphere models predict that the spectral energy distribution of giant gas planets peaks beyond ~4-5 µm (M band), a spectral region strongly affected by very high background on ground-based telescopes. The spectral region beyond ~2.5 µm is thus a unique discovery space for JWST both for exoplanet detection and characterization. Table 1 shows the expected planet/star contrast for various combinations of companion mass, age and stellar mass primary (spectral type). The table is color coded to highlight regions of the parameter space accessible with TFI for two notional angular separations (1" and 5") illustrative of a relatively distant (~50-100 pc) and nearby (<10 pc) sample.

By the time JWST is launched, next generation planet finder instruments on Gemini (Gemini Planet Imager; Macintosh et al 2006) and VLT (SPHERE; Dohlen et al 2006)

should have found several tens of gas giant planets. The majority of these planets should be relatively massive (> 5 M_J), around relatively young (< 10-500 Myrs) FGK primaries in local associations (<10-100 pc) and should have separations between ~0.2" and 2". As seen in Table 1, all companions to FGK stars at separations beyond ~1" should be detectable with TFI and NIRCam provided a modest 10x speckle-noise attenuation is achieved through PSF calibration. This analysis conservatively ignores any contrast gain that may be obtained through MWI with TFI and NIRcam.

Figure 9: TFI coronagraphic simulation at 4.6 μm of a 100 Myr-old M0V star, notionally at a distance of10 pc, with a 1 M_J companion at 1" (10 AUs). The exposure time is the cumulative sum of 1 hr..

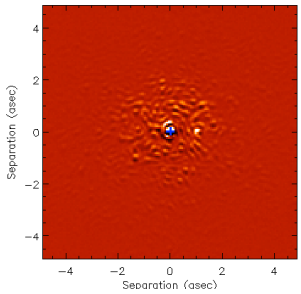

Vega is suspected to harbour a gas giant planet with an estimated mass ranging from 0.05 M_J (Neptune size) to 3 M_J. Very high-contrast *H*-band observations on Gemini (Marois et al 2006) already excludes a 3 M_J planet at 7-8" from Vega. Improving this limit further to ~1 M_J and smaller separations will be extremely challenging not to say impractical for extant ground-based telescopes. JWST will be particularly sensitive to low-mass gas giant planets at relatively large (>5") separations. As shown in Table 1, a 1 M_J planet could be detected beyond 5" around A0V stars.

The population of nearby young stars discovered in the last ~5 years (e.g Zuckerman & Song 2004) represents only a small fraction of the whole population. Many more late-type stars later than ~M4-M5 have yet to be discovered. On-going large scale surveys (UKIDSS, VISTA, PAN-Stars, SIMP), and in particular WISE, will find those stars through proper motion and follow-up observations. Most of these stars will be too faint for extreme AO planet finder instruments and laser guide stars will provide only modest corrections in a relatively high background. As seen in Table 1 and Figure 9, JWST will be capable of detecting 1 M_J planets around young (<100 Myrs) late type M stars. Table 1 also shows that JWST will detect 1 M_J companions around BDs without coronagraphy. Many of these companions will be Y dwarfs. Those objects will be particularly well suited for detailed spectroscopic investigations with the NIRSpec IFU since coronagraphy will not be required to detect them.

5.0 MIRI

MIRI is JWST's mid-infrared imager, and incorporates two coronagraphic imaging architectures. Figure 10 shows the coronagraphic focal plane mask assembly, which comprise three different quadrant phase masks (QPM), and a traditional coronagraphic occulting spot. Each of these focal plane masks images to a different pupil mask and filter combination. The three QPMs map to filters with central wavelengths of 10.65 μm, 11.4 μm and 15.5 μm ($\lambda/\delta\lambda \sim 20$), while the Lyot coronagraph pupil maps to 23 μm ($\lambda/\delta\lambda \sim 5$). The primary benefit

Figure 10: MIRI coronagraphic focal plane mask assembly. The first three mask apertures from the left are quadrant phase plates, while the final mask on the right is a traditional occulting spot.

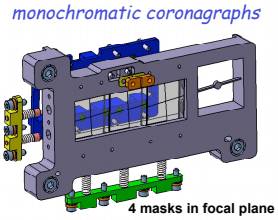

Figure 11: Detection limits for JWST, overplotted on spectra of EGPs from Allard et al. (2001).

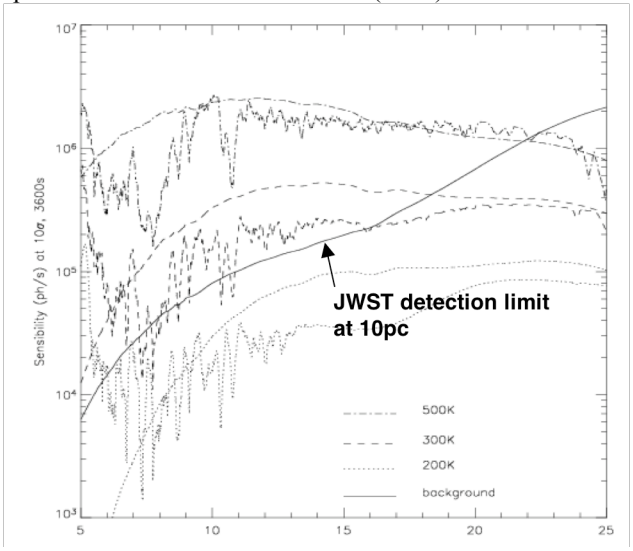

of using the quadrant phase mask concept for MIRI is that it provides a good inner working angle and contrast. Note that the primary concern associated with the quadrant phase technique, its sensitivity to pointing is negated for MIRI, because JWST's pointing far exceeds that needed for mid-IR imaging and is driven by JWST's near-IR image quality requirements. In addition to its coronagraph complement, MIRI also features an integral field spectrometer and will be able to conduct speckle deconvolution imaging programs in a similar way to that discussed in Section 4 for the Tunable Filter Imager.

MIRI will be able to detect gas giant planets with a broad range of characteristics. In Figure 11, we show the MIRI detection limit, for a range of extrasolar giant planet spectra computed by France Allard. These detection limits are compared in Figure 12 with the detection limit for a 30-m ground-based telescope. Much of MIRI's planet imaging capability will be complementary with the performance of NIRCam and the TFI. This is also the case for studies of planetary system formation. MIRI will be able to image debris disk systems in thermal emission, complementing reflected light images from the near-IR. MIRI will also to obtain mid-infrared spectra using the integral field unit.

Figure 12: Signal to noise ratio of EGPs as a function of the radial separation assuming a system located at 10 pc around an M2V star. The dotted and solid lines correspond respectively to the signal to noise ratio in the first and the second filters (ammonia absorption)

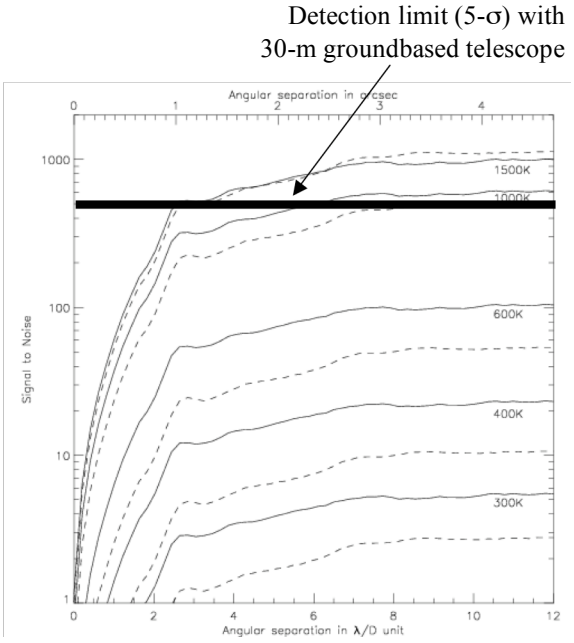

6.0 Summary

JWST has a wide range of capabilities for high contrast imaging by means of coronagraphy in the near to mid-infrared, and speckle deconvolution by means of integral field spectroscopy and tunable filter imaging that provide it with unique discovery space for exoplanet science.